PHYSICAL REVIEW D

PARTICLES AND FIELDS

THIRD SERIES, VOLUME 46, NUMBER 9 1 NOVEMBER 1992

RAPID COMMUNICATIONS

Rapid Communications are intended for important new results which deserve accelerated publication, and are therefore given priority in editorial processing and production. A Rapid Communication in **Physical Review D** *should be no longer than five printed pages and must be accompanied by an abstract. Page proofs are sent to authors, but because of the accelerated schedule, publication is generally not delayed for receipt of corrections unless requested by the author.*

Differential cross sections for dielectron production in distant ultrarelativistic heavy-ion collisions

N. Baron and G. Baur

Institut für Kernphysik (Theorie), Forschungszentrum Jülich, W-5170 Jülich, Germany

(Received 13 April 1992)

Singles angular distributions of electrons (positrons) are calculated for distant ultrarelativistic heavy-ion collisions. These QED pairs constitute a potential hazard for future detectors at relativistic heavy-ion colliders. We present numerical results in the relevant energy and angular ranges. The physics can be discussed transparently in terms of an easy to handle analytical formula.

PACS number(s): 25.75.+r, 13.40.Ks

It is well known that e^+e^- pairs are copiously produced via the γ-γ mechanism in nucleus-nucleus collisions at high energies [1] (for a recent paper with further references see Ref. [2]). There are plans to inject heavy ions such as Pb in the CERN Large Hadron Collider (LHC). The e^+e^- pairs produced by the γ-γ mechanism are a potential hazard for detectors at such machines [3]. It is therefore very important to provide a reliable assessment of these contributions to the dilepton spectra. This is the purpose of the present communication.

The production of dielectrons in the process

$$Z+Z\rightarrow Z+Z+e^+e^- \tag{1}$$

is mainly due to the γ-γ subprocess

$$\gamma+\gamma\rightarrow e^+e^- . \tag{2}$$

The photons in Eq. (2) can be described by the equivalent photon method (Weizsäcker-Williams approximation, see, e.g., Refs. [4,5]). One can view these photons as "partons" being present in fast moving charged particles; the equivalent photon spectrum corresponds directly to the "photon distribution function." The equivalent photon spectra for pointlike particles of charge Z are given by

$$n(\omega)=\frac{2}{\pi}Z^2\alpha\left[\frac{c}{v}\right]^2\left[\xi K_0(\xi)K_1(\xi)-\frac{v^2\xi^2}{2c^2}[K_1^2(\xi)-K_0^2(\xi)]\right], \tag{3}$$

where the Lorentz factor is given by $\gamma=[1-(v/c)^2]^{-1/2}$ with the ion velocity v and $\xi=\omega R/\gamma v$. The choice of the cutoff radius R has to be discussed very carefully: The basic assumption of the equivalent photon method is to treat the photons in the subprocess Eq. (2) as quasireal. Since low invariant mass e^+e^- pairs contribute predominantly, a realistic choice is $R\cong 1/m$, where m is the mass of the electron. This is also in accordance with the discussion of the limitations of the equivalent photon method in Refs. [6,7] (see especially Eq. 6.25 of Ref. [6]).

We want to calculate the differential e^+e^- production cross section in the c.m. system of the heavy ions (which coincides with the laboratory system for a collider). Since the energies ω and ω' of the corresponding colliding photons are in general different, the c.m. of the subsystem does not coincide with the heavy-ion c.m. system (see Fig. 1). Instead of performing the corresponding Lorentz transformations it is more convenient to deal with Lorentz-invariant formulations of the cross section. The differential cross section for the $\gamma\gamma\rightarrow e^+e^-$ reaction is given by (see, e.g., Ref. [8])

$$d\sigma_{\gamma\gamma}=\frac{\alpha^2}{2\omega\omega'}\frac{1}{\varepsilon_+\varepsilon_-}\left\{\frac{2\omega\omega'-m^2+(\omega\omega'-m^2)\sin^2\Theta}{m^2+(\omega\omega'-m^2)\sin^2\Theta}-\frac{2(\omega\omega'-m^2)^2\sin^4\Theta}{[m^2+(\omega\omega'-m^2)\sin^2\Theta]^2}\right\}\delta(\omega+\omega'-\varepsilon_+-\varepsilon_-)d^3\mathbf{p}_+ . \tag{4}$$

We can safely neglect the transverse momenta of the equivalent photons to establish the kinematical relation

$$\omega'=\frac{\omega(\varepsilon_+-p_+\cos\Theta)}{2\omega-\varepsilon_+-p_+\cos\Theta} , \tag{5}$$

where Θ is the positron scattering angle and ε_+, p_+ are the energy and the momentum of the positron in the laboratory system.

In the equivalent photon approximation we obtain, for the process (1),

$$d\sigma_{AA}=\int\frac{d\omega}{\omega}\frac{d\omega'}{\omega'}n(\omega)n(\omega')d\sigma_{\gamma\gamma} . \tag{6}$$

We insert Eqs. (4) and (5) into Eq. (6); the integration over ω' can be carried out directly with the help of the energy-conserving δ function. This leads to our final formula

$$\frac{d^2\sigma_{AA}}{d\varepsilon\,d\Omega}=\frac{\alpha^2}{2}p\int_{\hat{E}/2}^{\infty}\frac{d\omega}{\omega^4}\frac{2\omega-\hat{E}}{\tilde{E}^2}n(\omega)n\left[\frac{\omega\tilde{E}}{2\omega-\hat{E}}\right]\times\left\{\frac{2\omega\omega'-m^2+(\omega\omega'-m^2)\sin^2\Theta}{m^2+(\omega\omega'-m^2)\sin^2\Theta}-\frac{2(\omega\omega'-m^2)^2\sin^4\Theta}{[m^2+(\omega\omega'-m^2)\sin^2\Theta]^2}\right\}_{\omega'=\omega\tilde{E}/(2\omega-\hat{E})} , \tag{7}$$

where we defined $\hat{E}=\varepsilon+p\cos\Theta$ and $\tilde{E}=\varepsilon-p\cos\Theta$ for convenience. We suppressed the index $+$, since Eq. (7) holds for both positrons and electrons equivalently. The integral over ω is carried out numerically. For $(\omega\omega'-m^2)\sin^2\Theta\gg m^2$ we may approximate the curly brackets in Eq. (7) by $(2-\sin^2\Theta)/\sin^2\Theta$ and find a simple analytical expression

$$\frac{d^2\sigma_{AA}}{d\varepsilon\,d\Omega}=Z^4\alpha^4\frac{8}{3\pi^2}\frac{p}{\varepsilon}\frac{1}{\varepsilon^3}\left[\ln\frac{\varepsilon_m}{\varepsilon}\right]^2\frac{2-\sin^2\Theta}{\sin^6\Theta} , \tag{8}$$

where $\varepsilon_m=0.68\gamma m$ and we assumed that the logarithm is only a slowly varying function of the energies. One may note that for $\varepsilon\ll\varepsilon_m$ one is not very sensitive to the choice of the cutoff parameter R in Eq. (3).

In Fig. 2 energy spectra of positrons (or equivalently electrons) from ^{208}Pb–^{208}Pb collisions at various angles ($\Theta=30°$, 60°, 90°) are shown for LHC conditions. In Fig. 2(a) we show the energy range $m<\varepsilon<20$ MeV. The spectra for all three values of Θ show a rather sharp peak close to threshold. For increasing values of Θ the peak position is shifted closer to the threshold and the decrease of the spectrum for higher energies is enhanced. The dashed line corresponds to a calculation using the analytical expression (8) for $\Theta=90°$. It should be noted that this approximation describes the full calculation

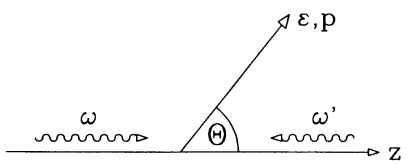

FIG. 1. The kinematics of pair production. The momenta of the colliding photons of energy ω and ω' are chosen in the beam direction (z axis); we neglect transverse momenta of the photons. The angle between the direction of the produced positron (or equivalently electron) and the positive z axis is denoted by the Θ.

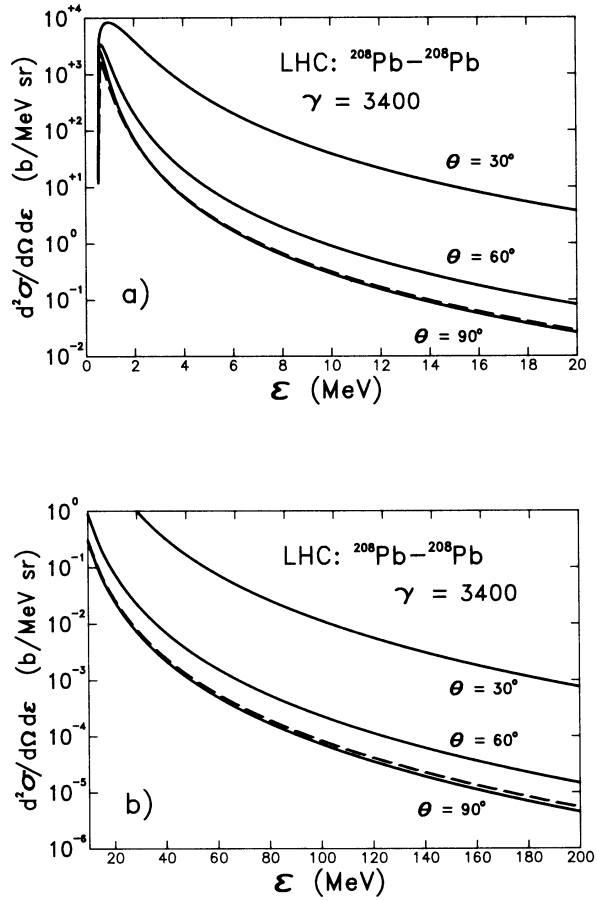

FIG. 2. Double differential cross section $d^2\sigma/d\Omega\,d\varepsilon$ for ^{208}Pb–^{208}Pb collisions at LHC conditions for fixed values of $\Theta=30°$, 60°, 90° as a function of the energy of the outgoing positron (electron). The full lines correspond to the full calculation of Eq. (7) while the dashed line corresponds to the analytical calculation of Eq. (8) for $\theta=90°$. (a) Energy range between threshold and 20 MeV. (b) Energy range between 10 and 200 MeV.

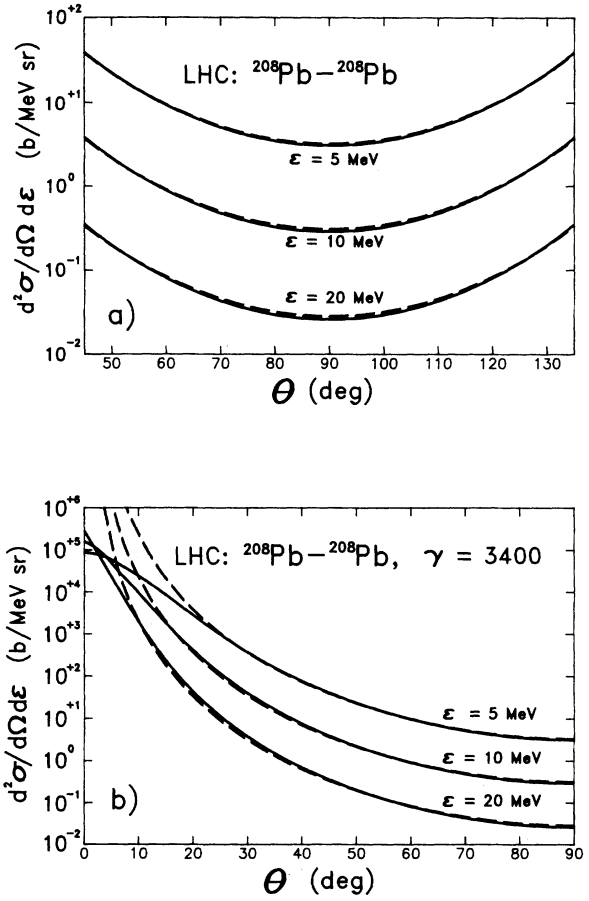

FIG. 3. Double differential cross section $d^2\sigma/d\Omega\, d\varepsilon$ for ^{208}Pb−^{208}Pb collisions at LHC conditions for fixed values of $\varepsilon=5$, 10, 20 MeV as a function of the angle Θ of the outgoing positron (electron). The full lines correspond to the full calculation of Eq. (7) while the dashed ones are due to the corresponding analytical calculations of Eq. (7). (a) Angular range between 45° and 135°. (b) Full angular range from 0° to 90°.

very well for energies between 2 and 10 MeV, while near threshold Eq. (8) clearly underestimates the full calculation. This is caused by the breakdown of the approximation for the curly brackets in Eq. (7). In Fig. 2(b) we show the energy range $10<\varepsilon<200$ MeV for the same angles Θ. All cross sections decrease very smoothly with increasing Θ. Again the dashed line corresponds to the calculation based on Eq. (8). In this energy region the analytical calculation overestimates the numerical one. This is due to the loss of accuracy in the approximation used to handle the equivalent photon spectra in deriving Eq. (8) from Eq. (7).

In Fig. 3 angular distributions for fixed values of the positron (or electron) energy ($\varepsilon=5$, 10, 20 MeV) are shown for ^{208}Pb−^{208}Pb collisions for LHC conditions. Figure 3(a) shows the angular distributions in an angular range between 45° and 135° relevant for a planned detector [3] at LHC. Although not manifest, it can be shown analytically from Eq. (7) that the distributions for fixed energies are symmetric around $\Theta=90°$ [in accordance with the numerical calculations of Fig. 3(a)]. For all values of the energies considered the distributions are shaped similarly, given approximately by the angular factor of Eq. (8). In Fig. 3(b) we show the full angular range from 0° to 90°. For all energies we obtain from the numerical calculation (full lines) the well-known peak for $\Theta=0°$ corresponding to the so called mass singularity (see, e.g., Ref. [9]). This peak is more pronounced at higher energies; for low energies the angular distributions become more and more flat. The dashed lines again correspond to the analytic calculation of Eq. (8) which is a very good approximation for all energies when angles larger than 20° to 30° are considered. For smaller angles the analytical solution would show a real singularity. This is a result of the approximation for the curly brackets in Eq. (7), which leads to the $1/\sin^2\Theta$ term. In the full formula (7) this singularity is removed by the finite value of the mass m of the created positron (electron).

Our results obtained by means of the equivalent photon method are a good approximation for small enough ε, i.e., $\varepsilon<\varepsilon_m=0.68\gamma m$. For $\gamma=3400$ this is $\varepsilon_m=1180$ MeV; i.e., it covers a large range of energies relevant for LHC detectors. For higher ε there are more sizable contributions due to closer collisions, $R\leq 1/m$. Nuclear form factors will also have to be taken into account for higher energies.

It was shown in Ref. [10] (see also Ref. [11]) that higher-order electromagnetic effects lead to the emission of multiple pairs in a single collision. However, this does not affect the final result, the rate of pair production. It was shown there that the perturbative result for one pair emission can become invalid for too small impact parameters ($b\cong 1/m$). Nevertheless it can be reinterpreted in terms of a Poisson distribution for multiple pair emission. The total number of dielectrons is unaffected.

For BNL Relativistic Heavy Ion Collider (RHIC) conditions ($\gamma=100$) we have $\varepsilon_m=34$ MeV, and our presently used approximation is only of restricted applicability. Nevertheless, due to the presence of the strong low-

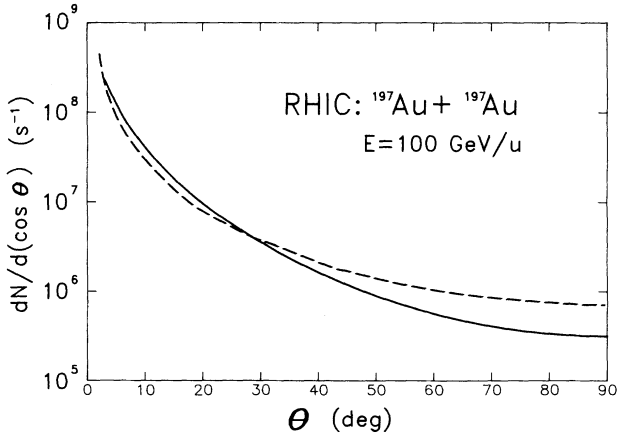

FIG. 4. Singles angular distribution $dN/d(\cos\Theta)$ [i.e., positron (electron) rate] as a function of the angle Θ for ^{197}Au−^{197}Au collisions at RHIC. The full line corresponds to our calculation while the dashed line shows the Monte Carlo calculation of Ref. [12]. A luminosity of $L=2\times10^{26}$ cm^{-2}s^{-1} was assumed.

energy peak, energy integrated cross sections can still be reliable. In Ref. [12] calculations on the e^+e^- background at RHIC for ^{197}Au–^{197}Au collisions are reported. These calculations were performed with a modified version of the Monte Carlo code [13]. For large values of the momenta our present methods are incomplete; however, for processes where low energies are involved we can compare our calculation with the result of Ref. [12].

In Fig. 4 we compare the singles angular distribution $dN/d(\cos\Theta)$ [i.e., the positron (electron) rate] of Ref. [12] (dashed line) with the present results (full line). In order to calculate this rate from our cross section we follow Ref. [12] and assume a luminosity of $L=2\times10^{26}$ $\mathrm{cm}^{-2}\mathrm{s}^{-1}$ for the Au^{79+} beam at RHIC. There is an overall agreement between the two calculations. Our angular distribution is somewhat steeper than the Monte Carlo calculation. The origin of this difference is not clear to us. We have seen that for $\varepsilon \gg m$ the angular distribution shows, with quite good accuracy, a $(2-\sin^2\Theta)/\sin^6\Theta$ behavior. For ε closer to threshold this distribution gets flatter, but not so flat as to lead to a closer agreement with the calculation of Ref. [12].

In conclusion, we have presented a transparent treatment of singles' angular distributions in e^+e^- production at ultrarelativistic heavy-ion colliders. These copiously produced pairs are a potential hazard for future detectors and it is important to have this QED background under control. Since we treat the photons as quasireal, we had to impose a cutoff on the equivalent photon spectra; this is expected to slightly underestimate the cross sections. For low electron energies (i.e., $\varepsilon \ll \varepsilon_m$) this is expected to be quite unimportant while for larger values of ε more elaborate calculations are needed.

Stimulating and helpful discussions with J. Schukraft (CERN) are gratefully acknowledged. One of the authors (N.B.) would like to thank the Studienstiftung des deutschen Volkes for the support of his studies.

[1] L. D. Landau and E. M. Lifschitz, Phys. Z. Sowjetunion **6**, 244 (1934).

[2] G. Baur and C. A. Bertulani, Nucl. Phys. **A505**, 835 (1989).

[3] J. Schukraft (private communication); in Proceedings of the General Meeting on LHC Physics and Detectors, Evian-les-Bains, France, 1992 (unpublished).

[4] J. D. Jackson, *Classical Electrodynamics* (Wiley, New York, 1975).

[5] C. A. Bertulani and G. Baur, Phys. Rep. **163**, 299 (1988).

[6] V. M. Budnev *et al.*, Phys. Rep. **15**, 181 (1975).

[7] C. Carimalo, P. Kessler, and J. Parisi, Phys. Rev. D **18**, 2443 (1978).

[8] A. I. Akhiezer and V. B. Berestetskii, *Quantum Electrodynamics* (Interscience, New York, 1965).

[9] T. D. Lee, *Particle Physics and Introduction to Field Theory* (Harwood Academic, New York, 1981).

[10] G. Baur, Phys. Rev. A **42**, 5736 (1990).

[11] M. J. Rhoades-Brown and J. Weneser, Phys. Rev. A **44**, 330 (1991).

[12] M. J. Rhoades-Brown, T. Ludlam, J.-S. Wu, C. Bottcher, and M. R. Strayer, in *Proceedings of the 4th Workshop on Experiments and Detectors for a Relativistic Heavy Ion Collider,* Upton, New York, 1990, edited by M. Fatyga and B. Moskowitz (BNL Report No. 52262, Upton, NY, 1991), p. 325; J.-S. Wu, M. J. Rhoades-Brown, C. Bottcher, and M. R. Strayer, Nucl. Instrum. Methods A **311**, 249 (1992).

[13] C. Bottcher and M. R. Strayer, Phys. Rev. D **39**, 1330 (1989).